Journal of Catalysis **189,** 221–232 (2000)
Article ID jcat.1999.2697, available online at http://www.idealibrary.com on IDEAL®

Titania–Silica Epoxidation Catalysts Modified by Polar Organic Functional Groups

C. A. Müller, M. Schneider, T. Mallat, and A. Baiker[1]

Laboratory of Technical Chemistry, Swiss Federal Institute of Technology, ETH Zentrum, CH-8092 Zurich, Switzerland

Received July 29, 1999; revised September 10, 1999; accepted September 28, 1999

Mesoporous titania–silica mixed oxides with covalently bound 3-chloropropyl, 3-acetoxypropyl, and *N*,*N*-dimethyl-3-aminopropyl groups were prepared from the corresponding alkyltrimethoxysilane and tetramethoxysilane using a sol–gel process and ensuing low temperature supercritical extraction with CO_2. The aerogels were characterized by thermal analysis, N_2 and NH_3 adsorption, infrared spectroscopy, and ^{29}Si and ^{13}C NMR spectroscopy. The modified aerogels showed reduced thermal stability compared to the unmodified titania–silica aerogel. Si–C bond breaking was detected already around 150°C. ^{29}Si MAS NMR measurements indicated covalent incorporation of the modifying group. DRIFT and NMR measurements confirmed the incorporation of 3-acetoxypropyl and *N*,*N*-dimethyl-3-aminopropyl groups and indicated the partial hydrolysis of 3-chloropropyl group to the corresponding alcohol. The activity in the epoxidation of cyclohexene and cyclohexenol with *tert*-butylhydroperoxide was significantly higher for 3-acetoxypropyl- and *N*,*N*-dimethyl-3-aminopropyl-modified catalysts than for the unmodified aerogel. Cyclohexenol oxide selectivity with the *N*,*N*-dimethyl-3-aminopropyl-modified catalyst was 94% at 91% peroxide conversion. The new aerogels are compared to other known Ti- and Si-containing epoxidation catalysts, including titania–silica mixed oxides modified by apolar functional groups. © **2000 Academic Press**

Key Words: **titania–silica hybrid gel; aerogel; organic modification; chloropropyltrimethoxysilane; acetoxypropyltrimethoxysilane; dimethylaminopropyltrimethoxysilane; epoxidation; cyclohexene; cyclohexenol; *tert*-butylhydroperoxide.**

1. INTRODUCTION

The possibility of modifying the surface of silicon based solids with organic groups via the thermally stable and relatively inert Si–C bond has been used extensively in the past decade (1). Well known examples are the advanced materials developed for chromatography and the immobilization of enzymes for industrial purposes. The use of organically modified solids as catalysts is limited by their thermal stability and thus restricted to liquid phase organic reactions (2, 3). The successful applications include reactions catalyzed by solid acids and bases, and oxidation catalysts (4–10). An important aspect of modification techniques is the possibility of immobilizing transition metal complex catalysts onto a silica surface (11–15), combining the advantages of heterogeneous and homogeneous catalysts.

Only recently has the influence of organic modification on the surface polarity and catalytic activity been studied for the epoxidation of olefins over titania–silica mixed oxides (16–18). The research activities so far have focused on the hydrophobization of the catalysts in order to facilitate the use of hydrogen peroxide as oxidant and thus mimic the outstanding properties of TS-1 (16–18). It was assumed that surface hydrophobization by introducing methyl and phenyl groups would prevent titanium from leaching when aqueous hydrogen peroxide was used as oxidant. Although this goal has been achieved, selectivities and activities were not satisfying (16, 17).

Mesoporous titania–silica mixed oxides dried by semicontinuous extraction with supercritical CO_2 have been shown to be excellent catalysts for the epoxidation of alkenes, alkenols, and alkenones with alkyl hydroperoxides (19, 20). The structure and activity of these aerogels was controlled by adjustment of the sol–gel preparation and drying procedure (21). Acidity of the mixed oxide is crucial for activating the peroxide, but can also result in acid catalyzed side reactions of reactants and products (22). Tuning the acidity with weakly basic organic and inorganic additives has been shown to considerably improve the performance of titania–silica mixed oxides (20, 22, 23). Especially amine addition was found to enhance the epoxide selectivities. Selectivities up to 98% in the demanding epoxidation of 3-methylcyclohex-2-en-1-ol were achieved with high reaction rates (20). The positive influence was explained by the neutralization of some acid sites present in the catalyst. The successful immobilization of a tertiary amine on a mesoporous titania–silica mixed oxide led to a recyclable, selective, and active catalyst for allylic alcohol epoxidations (20).

---

[1] To whom correspondence should be addressed. Fax: +41 1 632 11 63. E-mail: baiker@tech.chem.ethz.ch.

0021-9517/00 $35.00

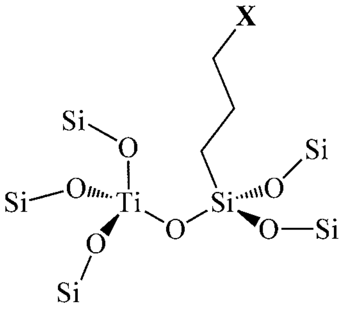

X = Cl, OAc, NMe$_2$

SCHEME 1. Schematic structure of targeted organically modified titania–silica mixed oxides.

Here we describe the synthesis of novel organically modified mesoporous titania–silica mixed oxides with a target structure as illustrated in Scheme 1. The aerogel synthesis followed a previously published route (18) but was changed significantly to compensate for the different sol–gel activities of the precursors. In contrast to the earlier strategy, outlined above, we aimed at introducing polar organic functional groups via Si–C bonds. The functional groups are supposed not only to change the surface properties with respect to polarity and acidity, but might also interact directly with the titanium active site as electron-donating ligands (24–26). The catalytic potential of these organically modified titania-silica aerogels is tested in the epoxidation of cyclohexene and cyclohexenol with *tert*-butylhydroperoxide. These substrates are assumed to interact differently with the active titanium sites (27–29).

2. EXPERIMENTAL

Catalyst Preparation

Acronyms used for the different catalysts are listed in Table 1 together with important information concerning the compositions of sol–gel solutions used in synthesis. The numbers in the abbreviations used for the catalysts indicate the percentage of modified silicon precursor based on the total amount of silicon. The aerogels were prepared according to procedures previously published (18, 21). Prehydrolysis of the precursor for CP30 (chloropropyltrimethoxysilane, CPTMS, Fluka ca. 97%) and ACOP10 (acetoxypropyltrimethoxysilane, ACOPTMS, ABCR) in *i*-PrOH with aqueous HNO$_3$ hydrolysant under vigorous stirring (1000 rpm) lasted 6 h. The prehydrolysis was necessary to compensate for the different sol–gel reactivities of the precursors (18, 30). Subsequently, tetramethoxysilane (TMOS; Fluka, puriss.) and titaniumbisacetylacetonatediisopropoxide (TIBADIP, 75% in *i*-PrOH; Aldrich puriss.) in *i*-PrOH were added. The titania loading of all aerogels was 10 wt% TiO$_2$ for a theoretical catalyst TiO$_2$–SiO$_2$. After 24 h, trihexylamine (THA, Fluka >97%) in *i*-PrOH was added and the stirring speed reduced (500 rpm). Gelation to an opaque monolithic body occurred within 1 h.

Different preparation conditions for the amine-modified aerogel had to be chosen because the amine precursor itself acts as a base catalyst. A solution of TMOS and TIBADIP in *i*-PrOH was mixed with the acidic hydrolysant. After 6 h, THA and *N*,*N*-dimethylaminopropyltrimethoxysilane (DMAPTMS, Fluorochem, 95%) in *i*-PrOH were added and gelation occurred immediately. All gels were aged for 7 days.

TABLE 1

Components Used for Sol–Gel Preparations[a]

Aerogel	*R* group in modifier precursor *R*–Si–(OMe)$_3$	Components added: At start	After 6 h	After 24 h	Theoretical TiO$_2$ content[b] (wt%)
CP30	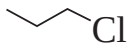	62 ml *i*-PrOH 45 mmol R–Si–(OMe)$_3$ 750 mmol H$_2$O 15 mmol HNO$_3$	10 ml *i*-PrOH 105 mmol TMOS 12.5 mmol TIBADIP	60 ml *i*-PrOH 22.5 mmol THA	7.6
ACOP10	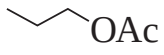	62 ml *i*-PrOH 15 mmol R–Si–(OMe)$_3$ 750 mmol H$_2$O 15 mmol HNO$_3$	10 ml *i*-PrOH 135 mmol TMOS 12.5 mmol TIBADIP	60 ml *i*-PrOH 22.5 mmol THA	8.8
DMAP10	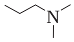	50 ml *i*-PrOH 750 mmol H$_2$O 15 mmol HNO$_3$ 135 mmol TMOS 12.5 mmol TIBADIP	82 ml *i*-PrOH 15 mmol R–Si–(OMe)$_3$ 22.5 mmol THA		8.9

[a] *i*-PrOH, 2-propanol; TMOS, tetramethoxysilane; TIBADIP, titaniumbisacetylacetonatediisopropoxide; THA, trihexylamine.

[b] Calculated by assuming that the amount of chemically bound water, present in SiOH groups, is zero.

Sol–gel processes were carried out in a glass reactor at room temperature under a He atmosphere. The total volume of the liquid was ca. 170 ml and the corresponding molar ratios water : silicon alkoxide : acid : THA were 5 : 1 : 0.1 : 0.15.

Semicontinuous extraction with supercritical CO_2 was carried out at 40°C and 230 bar. A glass liner was used to prevent contamination originating from the steel autoclave. The as-prepared aerogel clumps were ground in a mortar and calcined in a tubular reactor with upward flow. Aerogel CP30 was calcined at 200°C, whereas for the less stable catalysts ACOP10 and DMAP10, 100°C were used. All samples were heated at a rate of 10°C min^{-1} in an air flow of 5 L min^{-1} and kept at the final temperature for 1 h. The calcination temperatures were chosen on the basis of thermal analytical investigations (see below).

The composition of the samples with regard to Si, Ti, and Fe was determined by inductively coupled plasma atomic emission spectroscopy (ICPAES). The Si to Ti ratio was nominal and the Fe content was below 0.01% (detection limit).

Thermal Analysis

Experiments were carried out on a Netzsch STA 409 thermoanalyzer equipped with a gas injector. The weight loss of the sample during heat treatment was followed by TG. Gases evolved during heating were monitored on-line with a Balzers QMG 420 quadrupole mass spectrometer connected to the thermoanalyzer by a capillary heated to ca. 200°C.

Nitrogen Physisorption

The specific surface area (S_{BET}), mean cylindrical pore diameter ($\langle d_p \rangle$), and specific desorption pore volume ($V_p(N_2)$), assessed by the BJH method, were determined by nitrogen physisorption at −196°C using a Micromeritics ASAP 2000 instrument. Prior to measurement, the sample was degassed at 100°C until a final constant pressure below 0.1 Pa was achieved. BET surface area was calculated in a relative pressure range between 0.05 and 0.2, assuming a cross-sectional area of 0.162 nm^2 for the nitrogen molecule. Pore size distribution was calculated applying the BJH method to the desorption branch of the isotherm (31).

FTIR Transmission Spectroscopy

FTIR measurements were performed on a Perkin Elmer series 2000 instrument. The sample wafer consisted of 100 mg dry KBr and ca. 1 mg calcined sample. The cell was purged with a small flow of oxygen during the measurements. Five hundred scans were accumulated for each spectrum, at a spectral resolution of 4 cm^{-1}.

Ti dispersion in the silica matrix was estimated using

$$R = \frac{S_{(\text{Si–O–Ti})}}{S_{(\text{Si–O–Si})}}, \qquad [1]$$

where $S_{(\text{Si–O–Ti})}$ is the deconvoluted area of the peak at ca. 940 cm^{-1} and $S_{(\text{Si–O–Si})}$ that at ca. 1210 cm^{-1} (21).

DRIFT Spectroscopy

Diffuse reflectance infrared Fourier transform spectroscopy was carried out on a Perkin Elmer series 2000 instrument. The sample was measured undiluted. Each sample was preheated in air to 200°C for CP30 and 100°C for ACOP10 and DMAP10 with a heating rate of 5°C min^{-1}. After cooling to 50°C, the background spectra were recorded at 50°C in air. The spectra were accumulated from 500 scans. The sample was flushed with Ar (0.5 h) and then with NH_3 (5% in Ar) for 0.5 h and finally again with Ar for 1.5 h. The DRIFT difference spectra were obtained by subtracting the corresponding background spectra from the spectra after NH_3 adsorption.

NMR Spectroscopy

For deconvolution of the T^2, T^3, Q^2, Q^3, and Q^4 MAS signals, starting values of −56, −64, −92, −100, and −109 ppm, respectively, were chosen. The peak position and the width of the peak were not fixed. Gaussian function was chosen for fitting and the fit was optimized using the least squares method.

Epoxidation Procedure

2-Cyclohexen-1-ol (Fluka, ca. 97%), cyclohexene (Fluka, >99.5%), and *tert*-butylhydroperoxide (TBHP; Fluka, ca. 5.5 M solution in nonane, stored over a 4-Å molecular sieve) were used as received. Toluene (Riedel-de Haën, >99.7%) was distilled and stored over a molecular sieve.

All reactions were carried out under purified He to avoid the presence of oxygen and moisture. In the standard procedure, 70 mg catalyst was transferred into a 50-ml glass reactor, equipped with a magnetic stirrer, thermometer, and reflux condenser and heated in a He flow to 200°C for 2 h (100°C for DMAP10 and ACOP10). After cooling to ambient temperature, 20 mmol of olefin or allylic alcohol, an internal standard (decane or pentadecane), and 2 ml of toluene (solvent) were added. The reaction was started at 90°C by addition of 5 mmol TBHP.

Samples were analyzed by an HP 6890 gas chromatograph (cool on-column injection, HP-FFAP column). Selectivities and yield were calculated as follows (the subscript 0 denotes initial concentrations):

- selectivity of the epoxide related to the olefin converted,

$$S_{\text{olefin}} = 100\% \frac{[\text{epoxide}]}{[\text{olefin}]_0 - [\text{olefin}]}; \qquad [2]$$

- selectivity of the epoxide related to the peroxide converted,

$$S_{\text{peroxide}} = 100\% \frac{[\text{epoxide}]}{[\text{peroxide}]_0 - [\text{peroxide}]}; \qquad [3]$$

- epoxide yield related to the peroxide,

$$\text{yield} = 100\% \frac{[\text{epoxide}]}{[\text{peroxide}]_0}. \qquad [4]$$

Note that the reactant/peroxide molar ratio was 4 : 1. The initial rate was defined as the epoxide formation in the first 5 min.

3. RESULTS

Textural Properties—Nitrogen Physisorption

The results of nitrogen physisorption measurements carried out on calcined materials are listed in Table 2. The corresponding pore size distributions and *t* plots are presented in Fig. 1. The BET surface areas (228–312 $m^2\,g^{-1}$) are lower than those obtained previously for unmodified titania–silica aerogels (500–700 $m^2\,g^{-1}$, (21)) and for methyl-modified titania–silica aerogels with 20 wt% TiO_2-loading (450–550 $m^2\,g^{-1}$ (18)). The methyl-modified aerogels containing 10–30% methylated silicon were prepared in a similar way, except the use of THA as gelation catalyst was not necessary. Introduction of polar functional groups obviously lowered the surface area accessible for nitrogen, but all samples are predominantly mesoporous.

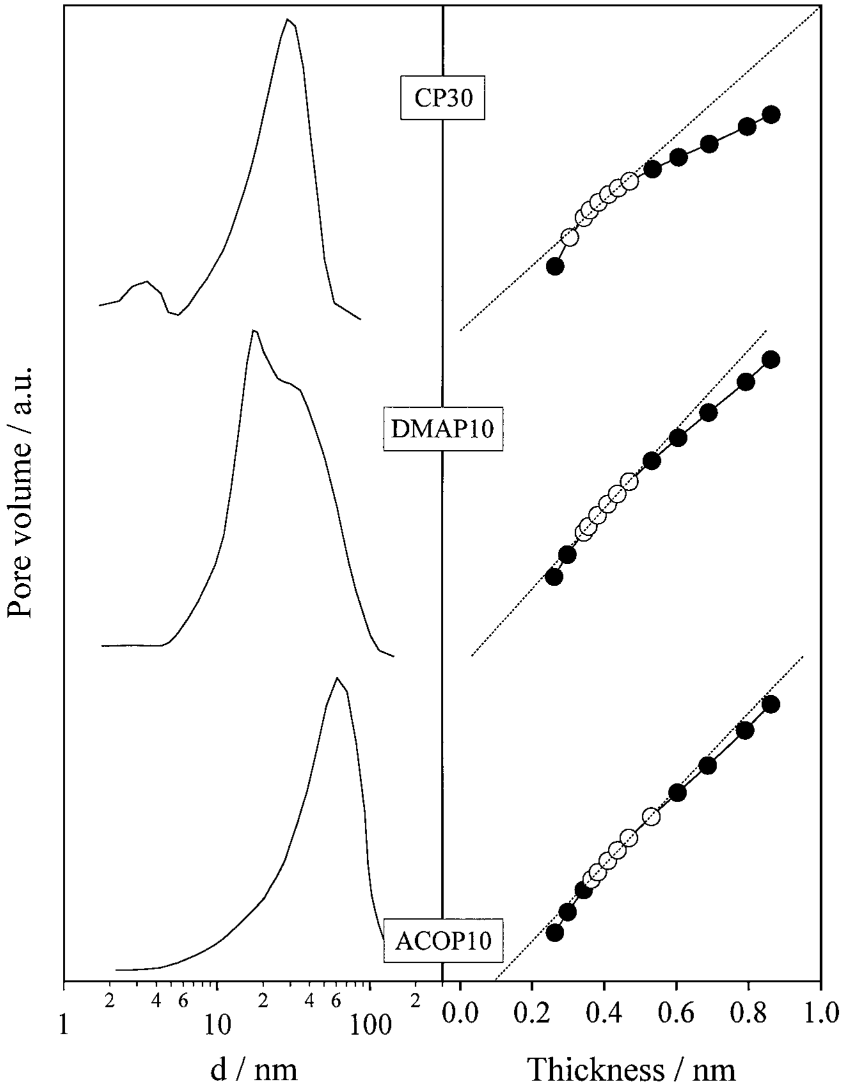

FIG. 1. Pore size distribution (left) and *t* plots (right), of organically modified aerogels, determined by N_2 adsorption.

TABLE 2

Physico-chemical Properties of the Aerogels

Aerogel	S_{BET} ($\mathrm{m^2\,g^{-1}}$)	$V_{\mathrm{p}}{}^{a}$ ($\mathrm{cm^3\,g^{-1}}$)	$V_{\mathrm{m}}{}^{b}$ ($\mathrm{cm^3\,g^{-1}}$)	$\langle d_{\mathrm{p}}\rangle^{c}$ (nm)	R^{d}
CP30	228	0.27	0.05	5.8	0.20
ACOP10	251	1.61	0	16.7	0.55
DMAP10	312	1.01	0	11.6	0.35

[a] Designates the BJH cumulative desorption pore volume of pores in the maximum range1.7–300 nm diameter.

[b] Micropore volume from *t* method analysis.

[c] $\langle d_{\mathrm{p}}\rangle = 4V_{\mathrm{p}}/S_{\mathrm{BET}}$.

[d] $R = \mathrm{S_{(Si\text{–}O\text{–}Ti)}}/\mathrm{S_{(Si\text{–}O\text{–}Si)}}$, determined from FTIR spectra.

The pore volume is significantly lower for the CP30 aerogel when compared to ACOP10 and DMAP10. This can be explained by the higher modifier loading (18). Concomitantly, only for CP30 a substantial micropore volume was indicated by the *t*-method analysis. The shape of the pore radii distribution for the CP30 material is similar to distributions previously published on chloropropyl-modified silica (32). Some microporosity is also reflected by the *t* plots in Fig. 1. The plot for CP30 shows a significant deviation from the fitted line for higher *t* values, an observation that can be explained by microporous domains (33). The average pore diameter calculated assuming cylindrical pores ($\langle d_{\mathrm{p}}\rangle$) is also considerably lower for CP30 than for ACOP10 and DMAP10. The pore size distribution of CP30 (Fig. 1) shows some pores in the lower range just above the analysis limit of the BET method (ca. 2 nm).

Ti Dispersion–FTIR Spectroscopy

Titanium dispersion is estimated by FTIR measurements. As a semiquantitative measure for the Ti dispersion, the ratio between the peak intensities of the Si–O–Ti vibration at 940–960 $\mathrm{cm^{-1}}$ and the Si–O–Si vibration around 1200 $\mathrm{cm^{-1}}$ has been established (21). The ratios are listed in Table 2. The CP30 aerogel has the smallest value with 0.20 which can be explained by a decreased titanium dispersion due to a large extent of organic modification (30%). This effect has been previously observed for methyl-modified titania–silica aerogels (18). However, distortion of the *R* values by contribution from other components, such as $\mathrm{Si\text{–}O^-}$ vibrations (34) or vibrations of the organic modification in the respective ranges cannot be excluded. Thus, the dispersion values in Table 2 should be considered as rough estimates.

Bulk Structure–^{29}Si NMR Spectroscopy

The bulk structure of the aerogels has been investigated by ^{29}Si MAS-NMR (no cross-polarization applied) and the results are presented in Table 3. Incorporation of organic modification is confirmed by the presence of signals corresponding to T sites (Si atoms bound to one carbon and three oxygen atoms; $T^2 = R\text{–Si(OH)(O–Si)}_2$, $T^3 = R\text{–Si(O–Si)}_3$) in the NMR spectra. The cumulative values of the *T* peak intensities were 20% (nominal 30%) for CP30, 13% (nominal 10%) for ACOP10, and 11% (nominal 10%) for DMAP10. Hence, NMR analysis corroborated the presence of organic functional groups in the aerogels anchored via Si–C bonds, but the estimated error of measurement and peak deconvolution was too high for a quantitative analysis.

As a measure for cross-linkage, the ratio of Q^4 ($\mathrm{Si(O\text{–}Si)_4}$) to Q^3 sites ($\mathrm{Si(OH)(O\text{–}Si)_3}$) has been used before (18), with higher ratios indicating stronger cross-linking. The highest ratio (1.8) was found in CP30. An even higher value $Q^4/Q^3 = 2.3$ has been found previously for a titania–silica aerogel possessing 30% methyl functional groups (18). The measurement confirms a stronger cross-linkage for titania–silica aerogels with higher amounts of incorporated organic functional groups. The ratios for ACOP10 (0.9) and DMAP10 (1.3) are also in accordance with those found for aerogels with 10% methyl-modified silicon ($Q^4/Q^3 = 1.4$) (18). The higher cross-linking in CP30 is well reflected by the lower BET surface area and average pore diameter, as compared to the other two aerogels (see Table 2).

Modification Structure–IR Spectroscopy

DRIFT spectra of the aerogels in air are depicted in Fig. 2. The left side shows the range from 4000 to 1000 $\mathrm{cm^{-1}}$, whereas in the right part the region around 2950 $\mathrm{cm^{-1}}$ is enlarged. In addition to the DRIFT spectra of the modified aerogels, the gas phase IR spectra of the compounds analogous to the immobilized modifier are also presented (*n*-propyl acetate, 1-chloropropane, *N*,*N*-dimethylaminopropane). Incorporation of organic functional groups led to additional signals on the titania–silica background. The peaks of the organic functions in the range 1500–1000 $\mathrm{cm^{-1}}$ overlap with large signals attributed to Si–O–Si, Si–O–Ti, and $\mathrm{Si\text{–}O^-}$ species. Elucidation of the structure of the organically modified aerogel is thus limited to the region 4000–1500 $\mathrm{cm^{-1}}$.

The spectra of ACOP10 and CP30 aerogels present peaks around 2950 $\mathrm{cm^{-1}}$ which correspond to signals of propyl acetate and 1-chloropropane, respectively (35). Both propyl acetate (Fig. 2, right c) and 1-chloropropane (Fig. 2, right a) display a signal at ca. 2975 $\mathrm{cm^{-1}}$ (C–H stretch vibration) that

TABLE 3

Structural Analysis by ^{29}Si MAS–NMR

Aerogel	Structural site T^2 (%)	T^3 (%)	Q^2 (%)	Q^3 (%)	Q^4 (%)	Q^4/Q^3
CP30	2	18	1	28	51	1.8
ACOP10	3	10	4	43	40	0.9
DMAP10	5	6	5	37	47	1.3

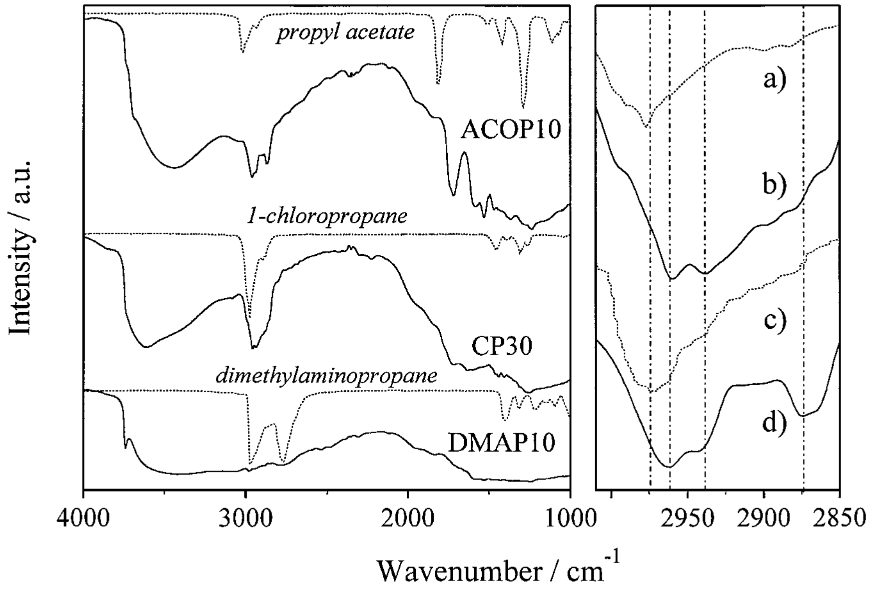

FIG. 2. (Left) DRIFT spectra of organically modified aerogels and FTIR spectra of the corresponding organic compound (from top down: *n*-propyl acetate, 1-chloropropane, *N*,*N*-dimethylaminobutane). (Right) Enlarged region 2850 to 3000 cm^{-1}; (a) 1-chloropropane, (b) CP30, (c) *n*-propyl acetate, (d) ACOP10.

seems to be slightly shifted to ca. 2960 cm^{-1} for ACOP10 (Fig. 2, right d) and CP30 (Fig. 2, right b). A shoulder in the ACOP10 spectrum at ca. 2940 cm^{-1} is not attributable to propyl acetate. A distinct peak which may be related to an ester carbonyl group is observed in the ACOP10 spectrum at ca. 1720 cm^{-1}. This signal is, however, shifted toward lower wavenumbers when compared to the propyl acetate spectrum (position at ca. 1810 cm^{-1}). A possible explanation for this shift is the interaction of the carbonyl O atom of the acetoxypropyl function with a neighboring silanol group, as H-bonding interactions lower the frequency of the carbonyl band (35).

Hydrolysis of the acetoxypropyl group is possible under sol–gel conditions. In order to elucidate a possible transformation of the organic function, spectra of ACOP10 before and after washing with tetrahydrofurane were compared. Hydrolysis would result in formation of acetic acid, which could account for the signal observed at ca. 1720 cm^{-1}. Acetic acid should be removed by careful washing. This signal was still present after the washing procedure (24 h, 60°C, reflux), which indicates the presence of unreacted acetoxypropyl functions at the surface. Nevertheless, hydrolysis of a small fraction of acetoxy groups during sol–gel synthesis cannot be precluded on the basis of IR measurements.

The typical strong and often broad bands of halogen compounds between 500 and 830 cm^{-1} (36) are not in the range of our DRIFT measurement. Less intensive signals in the range 1000 to 1500 cm^{-1} are concealed by strong matrix bands. Transmission FTIR measurements of CP30 did show peaks in the region below 850 cm^{-1} besides signals also observed for a reference catalyst with 30% methyl modification previously investigated (18) (Fig. 3, box). Since the methyl-modified aerogel did contain only methyl groups, the signals below 850 cm^{-1} in the CP30 spectrum are attributed to chloro-containing species. However, the low intensity of these additional peaks hinders any unambiguous interpretation.

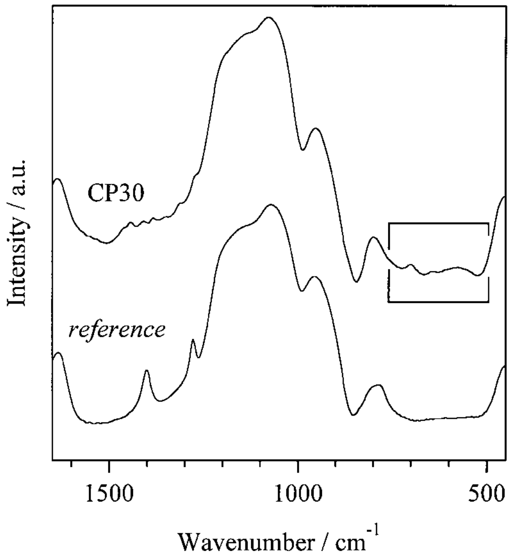

FIG. 3. Transmission FTIR spectra of chloropropyl-modified aerogel CP30 (top) and a 30Ae aerogel previously prepared (18) with 30% methyl modification as a reference (bottom).

The DMAP10 aerogel shows no clear evidence for signals typical for dimethylamino compounds. Only very small peaks in the region around 3000 and 2760 cm^{-1} are observed. Previous studies on dimethylaminopropyl-modified silica (37) reported the expected peaks at 2960 cm^{-1} (C–H$_{\mathrm{st}}$), 2760 cm^{-1} (N-(CH$_3$)$_{\mathrm{st}}$), and 1480 cm^{-1} (C–H$_{\mathrm{def}}$). Since ^{29}Si NMR confirmed the incorporation of organic modification for DMAP10, it seems that the concentration of the modifier is too small at the surface probed by DRIFT spectroscopy.

Ammonia Adsorption

Adsorption of ammonia on the catalysts has been investigated with DRIFT. The difference spectra of catalysts before and after ammonia adsorption are depicted in Fig. 4. The most striking difference between the catalysts is the outstanding ability of CP30 to adsorb ammonia, as evidenced by the higher intensity of the difference spectra. This is an indication that during sol–gel synthesis the chloropropyl functional groups—at least partly—hydrolyzed and the resulting hydrochloric acid was retained by the matrix. Note that trihexylamine (used to force gelation) is a good catalyst for dehalogenation. On the other hand, the very weak acidity of ACOP10 suggests that the acetoxypropyl function mostly preserved its integrity during catalyst preparation. The expected hydrolysis by-product acetic acid should result in significant enhancement in NH$_3$ adsorption.

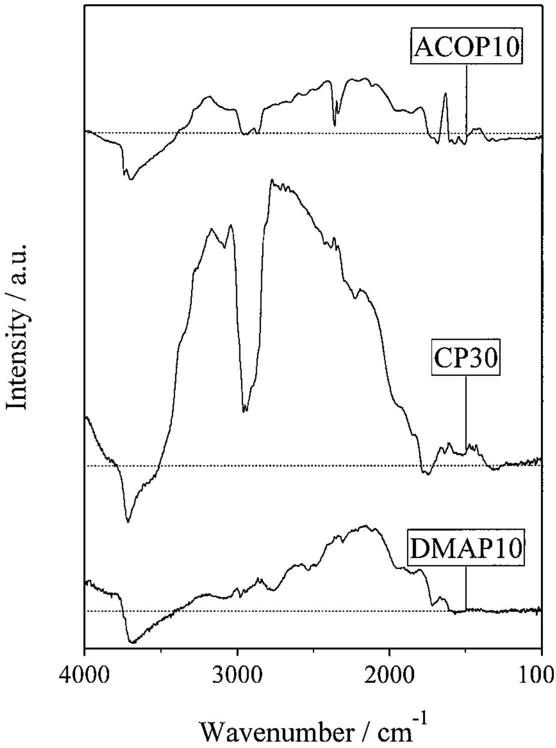

FIG. 4. DRIFT difference spectra (ammonia adsorption) for organically modified aerogels.

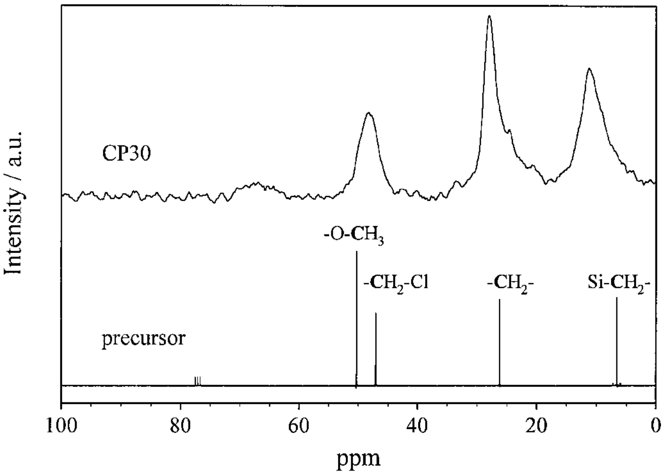

FIG. 5. Solid-state ^{13}C NMR of the aerogel CP30 (top) and ^{13}C NMR of 1-chloropropyltrimethoxysilane precursor (bottom).

Characteristic negative bands at ca. 3700 cm^{-1} are attributed to vanished Si–OH sites (38). Strong negative bands relative to the background of ammonia at ca. 2950 cm^{-1} (Fig. 4, ACOP10 and CP30) have previously been attributed to covered C–H bands for methyl-modified aerogels (18).

Modifier Structure–^{13}C NMR Spectroscopy

The ^{13}C NMR spectrum of CP30 is shown in Fig. 5 together with the spectrum of the corresponding precursor containing the organic functional group (chloropropyltrimethoxysilane). The good correlation between the spectra indicates that the organic modification is mainly present in the chlorinated form. The peak of the C atom bound to Si is shifted to higher frequencies probably due to incorporation into the solid matrix. The spectrum of the aerogel correlates well with the NMR data of chloropropyl-modified silica gels (39). The only exception is the broad and weak peak around 68 ppm which may indicate that a fraction of the chloropropyl functional groups hydrolyzed to hydroxy-propyl during the sol–gel synthesis (shift of α-C in propanol: 63.6 ppm (35)). No other peaks due to residues from the synthesis are apparent.

The spectrum of ACOP10 (Fig. 6) shows a multitude of peaks that are not assignable to the organic modification alone. The peak at ca. 11 ppm (No. *1*), in analogy to the CP30 spectrum, corresponds to the signal of the C atom bound to silicon. The peak at ca. 16 ppm (No. *2*) may be attributed to trihexylamine (THA gelation catalyst, spectrum also presented in Fig. 6). The peak at ca. 25 ppm (No. *3*) is probably the sum of several peaks of both the organic modification and the amine base. Peaks at ca. 28 and 34 ppm (Nos. *4* and *5*) originate from trihexylamine (C-2 and C-3 of the alkyl

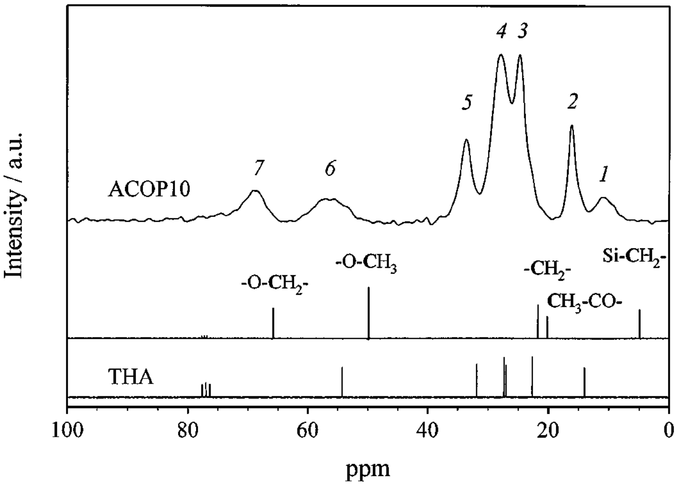

FIG. 6. Solid-state ^{13}C NMR of the aerogel ACOP10 (top) and ^{13}C NMR of acetoxypropyltrimethoxysilane precursor (middle) and trihexylamine gelation catalyst (bottom).

chain). The broad peak at ca. 57 ppm (No. *6*) is probably an overlapping of signals from both trihexylamine and the organic function, whereas the peak at ca. 69 ppm (No. *17*) is attributable to the modifier function. Note that corresponding peaks are missing in the trihexylamine spectrum. In the region between 170 and 200 ppm (not shown), two large signals which were assigned to carbonyl groups, stemming from acetylacetone (complexing agent of the titanium precursor), unhydrolyzed modifier precursor, or acetic acid, were observed. The ^{13}C NMR analysis thus confirms that incorporation of organic groups was successful. However, due to the moderate calcination temperature (100°C), a significant amount of organic residues stemming from the sol–gel process is still present in the catalyst.

A similar picture emerges for DMAP10 (Fig. 7). Some peaks are attributable only to residual trihexylamine (at ca. 26 ppm) and acetylacetone (at 170 and 200 ppm). On the other hand, the peak at ca. 45 ppm can be assigned unambiguously to the dimethylamino-modification of silica (no peak in this region in the trihexylamine spectrum, Fig. 6). Besides, no indication for a structural change of the modifying functional group upon sol–gel synthesis is observed.

TABLE 4

Epoxidation of Cyclohexene in Toluene with TBHP at 90°C

Aerogel	Initial rate (mmol g^{-1} min^{-1})	Yield after 2 h (%)	S_{olefin} after 2 h (%)	S_{peroxide} after 2 h (%)
CP30	1.8	—[a]	—	—
ACOP10	8.1	90	97	90
DMAP10	3.1	75	96	86

[a] Not determined, see text.

Catalytic Activity—Epoxidation of Cyclohexene and Cyclohexenol

The catalytic performance of organically modified aerogels was tested in the epoxidation of two bulky substrates with *tert*-butylhydroperoxide (TBHP) under dry conditions. The kinetics of the formation of epoxide and some by-products in the first 2 h was followed by GC analysis.

The results of the epoxidation of cyclohexene are presented in Table 4. All catalysts were active in epoxidation, but over CP30 the product cyclohexene oxide is consumed to significant extent by consecutive reactions. The kinetic curves resulting from the formation and decomposition of cyclohexene oxide are shown in Fig. 8. The major consecutive reaction over CP30 is the acid-catalyzed alcoholysis with *t*-BuOH coproduct (Scheme 2). Only a negligible amount of glycol was formed by ring opening with water.

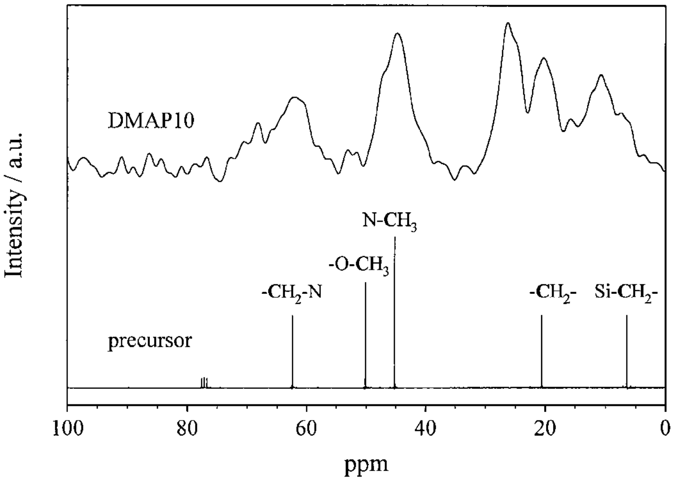

FIG. 7. Solid-state ^{13}C NMR of the aerogel DMAP10 (top) and ^{13}C NMR of *N*,*N*-dimethylaminopropyltrimethoxysilane precursor (bottom).

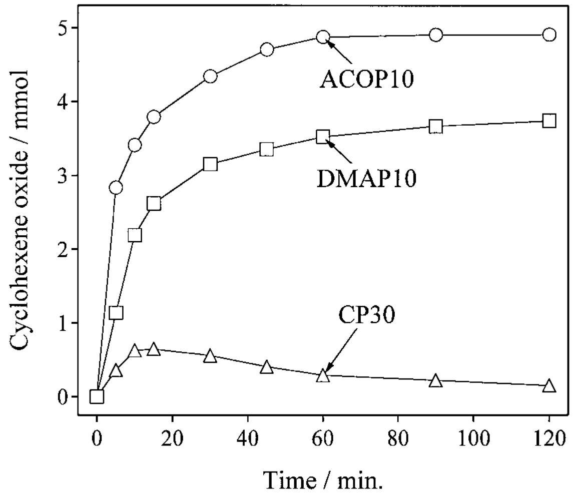

FIG. 8. Kinetic curves of cyclohexene oxide formation (and decomposition) with modified aerogels, at 90°C.

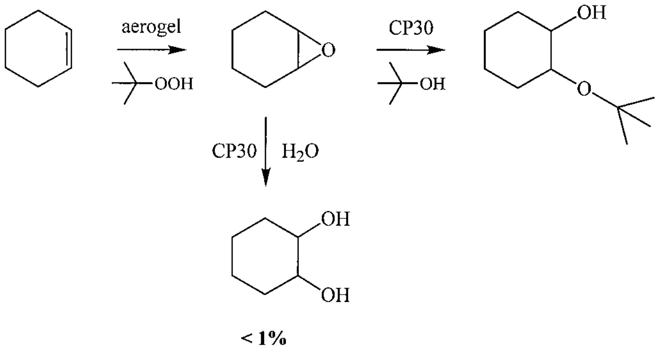

SCHEME 2. Ring opening reactions of cyclohexene oxide during epoxidation.

The appearance of water in the carefully dried reaction mixture may be attributed to dehydration of the *t*-BuOH coproduct, the reaction of which is also acid-catalyzed (40), or to formation of water by condensation of silanol groups (41). Due to the rapid consecutive reactions, no yield and selectivities were calculated for this catalyst. Both ACOP10 and DMAP10 catalysts were highly selective even at 90°C, which is not unusual in this facile reaction (19). It is evident from Table 4 that the yield for ACOP10 is limited by the peroxide selectivity only; i.e., the reaction stopped after 1 h (Fig. 8) when all TBHP was consumed.

The catalytic behavior of CP30 in the epoxidation of cyclohexenol with TBHP is entirely different from that observed in the epoxidation of cyclohexene (Table 5). No prevailing consecutive reaction of cyclohexenol oxide was observed, and the epoxide formed with 81% olefin selectivity at 81% peroxide conversion. Besides, this catalyst afforded the highest peroxide selectivity (83%). Interestingly, all three modified aerogels exhibited approximately the same initial activity for the epoxidation of cyclohexenol and cyclohexene (Tables 4 and 5). This is surprising because allylic alcohol epoxidation has been found to be a considerably more demanding reaction with respect to selectivity and activity when using unmodified titania–silica aerogels (23, 42). Due to the high activity of ACOP10 and DMAP10, the yields are limited only by the peroxide selectivity. The 93% olefin selectivity of DMAP10 at 75% olefin conversion (after 2 h reaction) is remarkably high. Major by-products are oligomers of substrate and cyclohexenol oxide, as well as the diether of cyclohexenol. The diastereomeric ratio (erythro/threo) in the epoxide is only marginally affected by the organic modification. For comparison, this ratio for an unmodified titania–silica aerogel was ca. 7 : 3, depending on the reaction conditions (42, 43). As concerns possible titanium leaching, the filtrated reaction mixture containing TBHP (without catalyst) did not show further chemical activity at 90°C.

4. DISCUSSION

Structural Analysis of Organically Modified Aerogels

The syntheses of three new, organically modified aerogels have been designed based on a sol–gel approach. Beside the general requirements for acceptable catalytic performance such as high surface area, mesoporous structure, and high abundancy of Ti–O–Si linkages (19), the silica network has to provide sufficient cross-linkage and thus stability within a reasonably low gelation time. These requirements were achieved by prehydrolysis of alkyltrimethoxysilane, tetramethoxysilane, and titaniumbisacetylacetonatediisopropoxide precursors under acidic conditions and subsequent forcing of the gelation with trihexylamine. The effect of base is probably the neutralization of positive charge located at the sol surface and thus the acceleration of the network building (30). During the preparation of DMAP10, the modification precursor dimethylaminopropyltrimethoxysilane (DMAPTMS) itself acted as catalyst together with trihexylamine (Table 1). Addition of DMAPTMS to the solution before prehydrolysis led to immediate precipitation. The same difficulty arose when more than 10% modified silicon precursor was attempted to be introduced, and in this case prehydrolysis could not solve the problem.

^{29}Si and ^{13}C NMR spectroscopy confirmed the incorporation of covalently bound organic moieties (X–$(CH_2)_3$–Si). However, spectroscopic characterization of the aerogels revealed some drawbacks of the acid- and base-catalyzed sol–gel route. IR spectroscopy showed that the chloropropyl functional groups partly hydrolyzed, presumably upon gelation forced by trihexylamine. The hydrolysis coproduct HCl was retained by the matrix and enhanced the acidity of this aerogel, as indicated by NH_3 adsorption measurement. It is likely that the exceptional textural properties of CP30 (lowest surface area, moderate pore diameter and Ti dispersion; small but significant microporosity, strongest

TABLE 5

Epoxidation of Cyclohexenol in Toluene with TBHP at 90°C

Aerogel	Initial rate (mmol g^{-1} min^{-1})	Yield after 2 h (%)	S_{olefin} after 2 h (%)	S_{peroxide} after 2 h (%)	Diastereomeric ratio after 2 h (%)
CP30	1.8	67	81	83	83 : 17
ACOP10	8.2	75	74	75	78 : 22
DMAP10	3.3	70	93	70	76 : 24

cross-linking) are also connected with this undesired side reaction and the partial neutralization of trihexylamine gelation catalyst. The poor performance of CP30 in cyclohexene epoxidation due to rapid consumption of cyclohexene oxide by acid-catalyzed consecutive reactions is further evidence for the partial degradation of the chloropropyl group.

Note that only few reports consider the synthesis of chloroalkyl-substituted Si-containing materials. Chloropropyl-modified silica was mostly produced by postmodification of silica with chloropropyltrialkoxysilane (39, 44, 45). The structural integrity of the chloropropyl-modification was confirmed by spectroscopic methods (39). Hüsing *et al.* (32) prepared chloropropyl-substituted silica aerogels via cocondensation of tetramethoxysilane and chloropropyltrimethoxysilane. Their characterization, however, did not elucidate the structure of the organic modification. Our results and the literature data indicate that either a more appropriate sol–gel route should be developed (by, e.g., substituting the N-base with another catalyst), or a postmodification method could be chosen.

To our knowledge, no reports have been published on modifications of silica or titania–silica with acetoxypropyl or hydroxypropyl groups. The acetoxypropyl group was chosen with the aim of producing hydroxypropyl-modified titania–silica via incorporation and hydrolysis in a one-step procedure, during the sol–gel synthesis. Hydroxyalkylsilanes are commercially not available, probably due to silylether formation of unprotected alcohols during synthesis. Astonishingly, the acetoxypropyl groups were stable during synthesis, despite the presence of acid or base in the aqueous alcoholic medium. No evidence for hydrolysis of the acetoxy group could be obtained by ^{13}C NMR as well as IR measurements. Besides, the low acidity of ACOP10 measured by NH_3 adsorption (Fig. 4) is also an indication for the preserved integrity of the ester functional group.

^{13}C NMR spectroscopy confirmed the incorporation of the dimethylaminopropyl groups in the DMAP aerogel as intended.

Catalytic Performance

Titania–silica catalysts have been extensively used in the epoxidation of olefins. Cyclohexene epoxidation is a frequent test reaction, since the accessibility of the catalytic sites can be assessed by the use of this bulky olefin. A notable property of the ACOP10 catalyst is the high epoxide selectivity (97%) combined with a high initial rate (8.1 mmol g^{-1} min^{-1}). Note that very high epoxide selectivities (up to 100%) are not unusual in this facile reaction (17, 19, 46).

On the other hand, epoxidation of allylic alcohols is more demanding and prone to numerous acid- and base-catalyzed side reactions (42). Table 6 provides a collection of data for the epoxidation of 2-cyclohexene-1-ol with various Ti- and Si-containing solid catalysts. The activity of the Shell catalyst (47), represented by the epoxide productivity (0.9 mmol g^{-1} h^{-1}), is rather low. The peroxide selectivity is yet surprisingly high (85%), when considering the 110°C reaction temperature and a 100% excess of oxidant. Interestingly, when changing the

TABLE 6

Epoxidation of Cyclohexenol with Ti- and Si-Based Catalysts

Catalyst	Oxidant	Time (h)	Temp. (°C)	Substrate/ oxidant ratio	Epoxide productivity[a] (mmol g^{-1} h^{-1})	S_{olefin} (%)	Peroxide conversion (%)	$S_{peroxide}$ (%)	Ref.
$TiCl_4$ grafted on SiO_2 (Shell)	TBHP	20	110	1 : 2	0.9	—	84	85	(47)
$Ti(O^iPr)_4$ grafted on SiO_2	TBHP	24	RT	3 : 2	—[b]	—	100	—	(49)
TS-1	H_2O_2	8	60	1 : 1.2	4	80	85	80	(28)
TiO_2–SiO_2 aerogel[c]	TBHP	1	90	4 : 1	39	65	83	67	(42)
Me-modified TiO_2–SiO_2 aerogel[d]	TBHP	1	90	4 : 1	70	95	—[e]	—	(18)
CP30	TBHP	1	90	4 : 1	35	80	60	82	
ACOP10	TBHP	1	90	4 : 1	53	82	97	76	
DMAP10	TBHP	1	90	4 : 1	46	94	91	70	

[a] Amount of epoxide formed per unit time and catalyst amount.
[b] Cyclohexenone was the only product.
[c] 20 wt% TiO_2–SiO_2, zeolite 4 Å as drying agent is added.
[d] 20 wt% TiO_2–SiO_2 with 10% methyl-modified silicon precursor.
[e] Peroxide conversion was not determined.

Ti precursor from $TiCl_4$ to $Ti(O^iPr)_4$, epoxide selectivity drops to zero and only the –OH function is oxidized to form cyclohexenone. Crystalline TS-1 (28) shows moderate activity (ca. 4 $mmol\,g^{-1}\,h^{-1}$) and good substrate (80%) and peroxide selectivity (80%). Very likely, the moderate activity has to be attributed to the oxidation of the bulky substrate at the outer surface of the microporous material. The TiO_2–SiO_2 aerogel is the closest reference material for the actual study, which catalyst has been prepared by a partly different procedure and does not contain organic functional groups. This aerogel is significantly more active than the Shell catalyst or TS-1, but concomitantly exhibits lower olefin (65%) and peroxide selectivities (67%). The experiments with CP30, ACOP10, and DMAP10 were conducted under exactly the same conditions to ensure direct comparison with the unmodified aerogel. The epoxide productivity of all three catalysts is similar or even better than that of the unmodified aerogel. The high epoxide productivity, which describes the average rate of epoxide formation, correlates well with the high initial activities shown in Table 5. A remarkable enhancement by organic modification has been achieved in the epoxide selectivity related to the olefin reaching a value of 94% for DMAP10 at 91% peroxide conversion. Only a methyl-modified titania–silica aerogel afforded higher olefin selectivity (98% after 10 min) and also higher average rate (productivity, Table 6), at comparable peroxide conversion. Note that the reactant-to-peroxide ratio in this work was higher compared to that used in the studies cited in Table 6.

Several advantages are thus realized by introducing organic functional groups to titania–silica catalysts. The materials combine the high activity of mesoporous titania–silica aerogels with high epoxide selectivities. Presumably due to the presence of some residue of trihexylamine, used as catalyst to force gelation, no addition of activated zeolite 4 Å during the epoxidation reaction is necessary to suppress acid-catalyzed side reactions (42). Furthermore, a reduction of TiO_2 content below 10 wt% is possible without loss of activity when compared to the unmodified aerogel possessing 20 wt% TiO_2 (42).

A challenging question is the correlation between the structural and catalytic data of organically modified titania–silica aerogels. A strong correlation between the semiquantitative value for the Ti dispersion determined by FTIR spectroscopy (*R* value, Table 2) and the catalytic activity has been observed for titania–silica aerogels (19). This correlation has been debated (48), pointing out that a contribution of Si–O^- species to the 960 cm^{-1} IR peak can seriously distort the evaluation of Ti–O–Si connectivity. Still, initial activity in this study seems again to be well correlated with the *R* value for the Ti dispersion (Tables 2, 4, and 5). We propose that despite the limitation of the method, a high *R* value is a good semiquantitative indicator for high density of isolated Ti sites and hence high epoxidation activity.

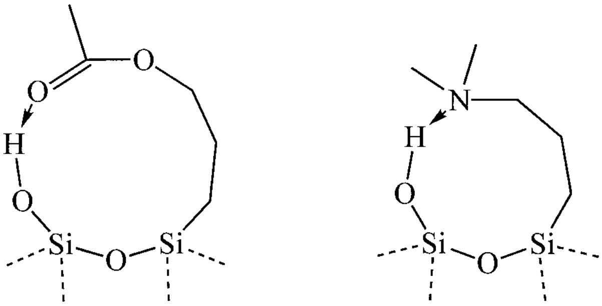

SCHEME 3. Possible H-bonding interactions of dimethylaminopropyl and acetoxypropyl functions with surface silanol groups.

An important requirement for high epoxidation activity and selectivity is the appropriate control of the acidity of the catalyst. In case of CP30 aerogel, a partial hydrolysis of the C–Cl bond during the sol–gel process is indicated by DRIFTS and ^{13}C NMR analysis. Due to the low calcination temperature (200°C) most of HCl produced may be retained by the solid, and it can act as a new acidic site during the epoxidation. This is the most probable explanation for the poor performance of CP30 in the oxidation of cyclohexene (Fig. 8).

On the other hand, DMAP10 contains basic functional groups, which can neutralize a part of surface silanol groups (Brønsted sites, Scheme 3). Similarly, H-bonding interaction of surface silanol groups with the electron-rich carbonyl O atom of the acetoxypropyl functional group (Scheme 3) is proposed to be a major reason for the good performance of the ACOP10 aerogel. The considerable shift of the carbonyl band of the acetoxypropyl function in the DRIFT spectrum of ACOP10, compared to that of propyl acetate, may indicate the $Si{-}OH\cdots O{=}C$ type interaction and can rationalize the suppression of acid-catalyzed side reactions during epoxidation.

Another point is the interaction of the acetoxypropyl and dimethylaminopropyl functional groups with the Ti active site. The electron rich carbonyl O and amino N atoms can act as electron donor ligands (24–26). This interaction is expected to tune the activity (acidity) of the Ti site. Unfortunately, we do not have yet an unambiguous evidence for this possibility.

5. CONCLUSIONS

A sol–gel route combined with ensuing extraction with supercritical CO_2 was applied to prepare titania–silica aerogels containing covalently bound polar functional groups. 3-Chloropropyl, 3-acetoxypropyl, and *N*,*N*-dimethyl-3-aminopropyl were introduced into the titania–silica by using corresponding alkyltrimethoxysilane precursors in the sol–gel process. NMR and vibrational spectroscopies confirmed that the acetoxypropyl and dimethylaminopropyl functions retained their integrity during sol–gel processing. In contrast, partial hydrolysis was observed with the 3-chloropropyl moiety, resulting in new acidic sites which lowered the epoxidation selectivity. A more selective gelation catalyst than trihexylamine is required to preserve the integrity of these functional groups.

Although all three catalysts were active and selective in the demanding epoxidation of 2-cyclohexen-1-ol, the dimethylaminopropyl-modified catalyst showed the best performance, achieving 93% selectivity at 100% peroxide conversion. The modification of TiO_2–SiO_2 epoxidation catalysts with polar functional groups is shown to be a promising strategy for tuning the properties of these catalytic materials.

ACKNOWLEDGMENTS

Financial support of our work by the ETH-Jubiläumsfond (TEMA-project) is gratefully acknowledged. Thanks are also due to Dr. M. Maciejewski for thermal analysis.

REFERENCES

1. Vansant, E. F., Voort, P. V. D., and Vrancken, K. C., *Stud. Surf. Sci. Catal.* **93**, 1 (1995).
2. Clark, J. H., and Macquarrie, D. J., *J. Chem. Soc. Chem. Commun.* 853 (1998).
3. Macquarrie, D. J., Clark, J. H., Jackson, D. B., Lambert, A., Mdoe, J. E. G., and Priest, A., *in* "Supported Reagents and Catalysts in Chemistry" (B. K. Hodnett, A. P. Kybett, J. H. Clark, and K. Smith, Eds.), p. 174. The Royal Society of Chemistry, Cambridge, 1998.
4. Butterworth, A. J., Clark, J. H., Walton, P. H., and Barlow, S. J., *J. Chem. Soc. Chem. Commun.* 1859 (1996).
5. Kurusu, Y., and Neckers, D. C., *J. Org. Chem.* **56**, 1981 (1991).
6. Barloy, L., Lallier, J. P., Battioni, P., Mansuy, P., Piffard, Y., Tournoux, M., Valim, J. B., and Jones, W., *New J. Chem.* **16**, 71 (1992).
7. Neumann, R., and Wang, T. J., *J. Chem. Soc. Chem. Commun.* 1915 (1997).
8. Clark, J. H., Martin, K., Teasdale, A. J., and Barlow, S. J., *J. Chem. Soc. Chem. Commun.* 2037 (1995).
9. Harmer, M. A., Sun, Q., Michalczyk, M. J., and Yang, Z. Y., *J. Chem. Soc. Chem. Commun.* 1803 (1997).
10. Angeletti, E., Canepa, C., Martinetti, G., and Venturello, P., *Tetrahedron Lett.* **29**, 2261 (1988).
11. McCann, M., Coda, E. M. G., and Maddock, K., *J. Chem. Soc. Dalton Trans.* **9**, 1489 (1994).
12. Kim, S. S., Zhang, W. Z., and Pinnavaia, T. J., *Catal. Lett.* **43**, 149 (1997).
13. Cai, M. Z., Song, C. S., and Huang, X., *Synth. Commun.* **28**, 693 (1998).
14. Kim, G. J., and Kim, S. H., *Catal. Lett.* **57**, 139 (1999).
15. Kröcher, O., Köppel, R. A., and Baiker, A., *J. Mol. Catal. A* **140**, 185 (1999).
16. Klein, S., and Maier, W. F., *Angew. Chem. Int. Ed. Engl.* **35**, 2230 (1996).
17. Kochkar, H., and Figueras, F., *J. Catal.* **171**, 420 (1997).
18. Müller, C. A., Maciejewski, M., Mallat, T., and Baiker, A., *J. Catal.* **184**, 280 (1999).
19. Hutter, R., Mallat, T., and Baiker, A., *J. Catal.* **153**, 177 (1995).
20. Dusi, M., Müller, C. A., Mallat, T., and Baiker, A., *J. Chem. Soc. Chem. Commun.* 197 (1999).
21. Dutoit, D. C. M., Schneider, M., and Baiker, A., *J. Catal.* **153**, 165 (1995).
22. Hutter, R., Mallat, T., Peterhans, A., and Baiker, A., *J. Mol. Catal. A* **138**, 241 (1999).
23. Dusi, M., Mallat, T., and Baiker, A., *J. Catal.* **173**, 423 (1998).
24. McAucliffe, C. A., and Bricklebank, N., *in* "Encyclopedia of Inorganic Chemistry" (R. B. King, Ed.), p. 4197. Wiley, Chichester, 1994.
25. Clark, R. J. H., *in* "Topics in Inorganic and General Chemistry" (P. L. Robinson, Ed.), p. 1. Elsevier, Amsterdam, 1968.
26. Mintz, E. A., *in* "Encyclopedia of Inorganic Chemistry" (R. B. King, Ed.), p. 4206. Wiley, Chichester, 1994.
27. Notari, B., *Adv. Catal.* **41**, 253 (1996).
28. Kumar, R., Pais, G. C. G., Pandey, B., and Kumar, P., *J. Chem. Soc. Chem. Commun.* 1315 (1995).
29. Adam, W., Corma, A., Martinez, A., Mitchell, C. M., Reddy, T. I., Renz, M., and Smerz, A. K., *J. Mol. Catal. A* **117**, 357 (1997).
30. Brinker, C. J., and Scherer, G. W., "Sol–Gel Science." Academic Press, Boston, 1990.
31. Broekhoff, J. C. P., *in* "Preparation of Heterogeneous Catalysts II" (B. Delmon, P. Grange, P. Jacobs, and G. Poncelet, Eds.), p. 663. Elsevier, Amsterdam, 1979.
32. Hüsing, N., and Schubert, U., *J. Sol.–Gel. Sci. Technol.* **8**, 807 (1997).
33. Baiker, A., and Kohler, M. A., *in* "Handbook of Heat and Mass Transfer" (N. P. Cheremisinoff, Ed.), p. 3. Gulf Pub., Houston, 1989.
34. Brodsky, C. J., and Ko, E. I., *J. Mater. Chem.* **4**, 651 (1994).
35. Silverstein, R. M., Bassler, G. C., and Morrill, T. C., "Spectrometric Identification of Organic Compounds." Wiley, New York, 1991.
36. Pretsch, E., Clerc, T., Seibl, J., and Simon, W., "Spectral Data for Structure Determination of Organic Compounds." Springer-Verlag, Berlin, 1989.
37. Mdoe, J. E. G., Clark, J. H., and Macquarrie, D. J., *Synlett* 265 (1998).
38. Liu, Z., Tabora, J., and Davis, R. J., *J. Catal.* **149**, 117 (1994).
39. Sudhölter, E. J. R., Huis, R., Hays, G. R., and Alma, N. C. M., *J. Colloid Interface Sci.* **103**, 554 (1985).
40. Sheldon, R. A., *in* "Aspects of Homogeneous Catalysis" (R. Ugo, Ed.), Reidel, Dordrecht, The Netherlands, 1981.
41. Iler, R. K., *in* "The Chemistry of Silica." Wiley, New York, 1979.
42. Dusi, M., Mallat, T., and Baiker, A., *J. Mol. Catal. A* **138**, 15 (1999).
43. Müller, C. A., Deck, R., Mallat, T., and Baiker, A., *Top. Catal.*, in press.
44. Tsubokawa, N., Kimoto, T., and Koyama, K., *Colloid Polym. Sci.* **271**, 940 (1993).
45. Menezes, M. L., Moreira, J. C., and Campos, J. T. S., *J. Colloid Interface Sci.* **179**, 207 (1996).
46. Chen, L. Y., Chuah, G. K., and Jaenicke, S., *Catal. Lett.* **50**, 107 (1998).
47. Wulff, H. P., patent, Shell Oil Company, USA, 1975.
48. Miller, J. B., Mathers, L. J., and Ko, E. I., *J. Mater. Chem.* **5**, 1759 (1995).
49. Cativiela, C., Fraile, J. M., Garcia, J. I., and Mayoral, J. A., *J. Mol. Catal. A* **112**, 259 (1996).